Functional Mitral Regurgitation

10

Timothy C. Tan, Xin Zeng, and Judy Hung

Abstract

Mitral valve regurgitation is one of the most common valve lesions. Clinical decision making for mitral regurgitation depends on accurate assessment of the mechanism and quantitation of mitral regurgitation. The mechanism of mitral regurgitation in a significant proportion of patients especially in the developed countries is functional. The mechanism underlying functional mitral regurgitation is due to left ventricular dilation. Furthermore, as functional mitral regurgitation is by nature a dynamic problem, accurate assessment of severity can be challenging. Echocardiography which enables real time imaging of the heart is the primary imaging modality in the diagnosis and assessment of functional mitral regurgitation. Important information can be obtained from a systematic echocardiographic assessment of the whole mitral apparatus and the underlying ventricular myocardium. Due to the complex spatial and dynamic pattern of flow across the mitral valve in patients with functional mitral regurgitation, obtaining accurate flow quantification using standard two-dimensional measures can be challenging. Three-dimensional echocardiographic techniques have been successful in overcoming some of the inherent geometric limitations of two-dimensional imaging. This chapter outlines the key aspects of functional mitral regurgitation and includes an overview of the anatomy of the mitral valve in the context of functional mitral regurgitation and standard flow measures as assessed using two- and three dimensional echocardiography.

Keywords

Mitral regurgitation · Functional · Ischemic Echocardiography · Severity · Three-dimensional echocardiography

Introduction

Mitral valve regurgitation is one of the most common valve lesions, representing nearly one-third of acquired left-sided valve pathology [1, 2]. This constitutes a significant disease burden considering that the prevalence of significant regurgitation (moderate to severe and severe) in the general population has been estimated at 2–3% and predicted to become increasingly more prevalent as the population ages [2]. Mitral regurgitation can arise from abnormalities in the function of the mitral valve which can be broadly classified into mitral regurgitation due to pathology or damage to the mitral valve leaflets or the associated valvular structures (primary mitral regurgitation); or mitral regurgitation due to left ventricular (LV) dilation resulting in failure of coaptation of the mitral valve leaflets without coexisting structural abnormalities of the valve or its associated valvular apparatus (functional mitral regurgitation, FMR). FMR, or secondary mitral regurgitation, makes up a large proportion of the cases of mitral regurgitation and has been independently associated with poor long-term survival, excessive morbidity and mortality. Hence, timely diagnosis and accurate grading of the severity of FMR are critical for appropriate patient management, particularly timing of surgical intervention [3–8]. Population studies also indicate that the incidence of FMR is expected to increase due to predicted demographic changes,

Electronic Supplementary Material The online version of this chapter (https://doi.org/10.1007/978-3-030-14032-8_10) contains supplementary material, which is available to authorized users.

T. C. Tan
Department of Cardiology, Westmead Hospital, Westmead, NSW, Australia
e-mail: tim.tan@sydney.edu.au

X. Zeng · J. Hung (✉)
Department of Medicine/Cardiology, Massachusetts General Hospital, Boston, MA, USA
e-mail: xzeng@mgh.harvard.edu; jhung@mgh.harvard.edu

L. P. Badano et al. (eds.), *Textbook of Three-Dimensional Echocardiography*, https://doi.org/10.1007/978-3-030-14032-8_10

progressively higher and longer survival to acute and chronic cardiac diseases affecting LV geometry and function. Factors such as an aging population and greater life expectancy, are expected to contribute to an increase in the incidence of ischaemic heart disease and dilated cardiomyopathy (the two most common causes of FMR) [2, 3].

FMR essentially results from failure of systolic coaptation of the mitral valve leaflets due to pathology affecting the LV. Most typically, the initiating insult relates to ventricular remodeling following myocardial infarction or ischemia, or dilated non-ischemic cardiomyopathy. Up to 40% of patients with heart failure caused by dilated cardiomyopathy are estimated to go on to develop FMR [9, 10]. Symptoms arising from FMR typically progresses slow and also often ends in contributing towards irreversible LV dysfunction.

Pathophysiology of Functional Mitral Regurgitation

FMR results from an altered force balance between tethering forces on the mitral leaflets from ventricular dilation and decreased closing forces (Fig. 10.1). With adverse LV remodeling that occurs with myocardial infarction or cardiomyopathy, the myocardium underlying the papillary muscles dilates and the mitral leaflets are pulled apically into the LV as a consequence of the outward displacement of the papillary muscles resulting from LV dilation. This results in increased tethering forces on the mitral leaflets resulting in incomplete mitral leaflet closure. Closing forces generated from LV contraction which act to close the leaflets are typically diminished in setting of LV cardiomyopathy and contribute to

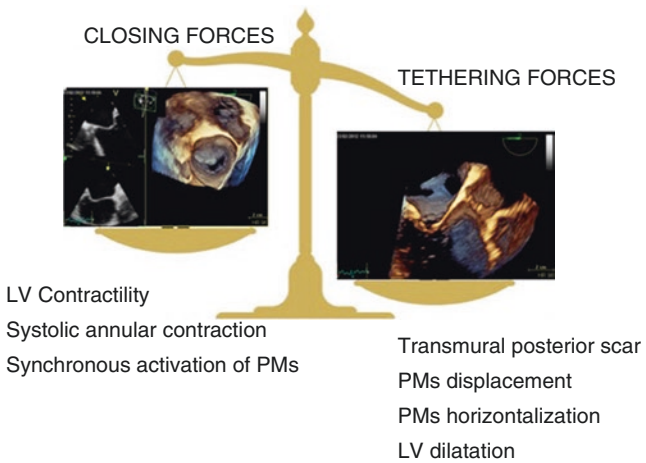

Fig. 10.1 Mechanism of functional mitral regurgitation. In patients with functional mitral regurgitation, the tethering forces on the mitral leaflets from ventricular dilation and or regional dysfunction prevail on the closing forces which are decreased. *LV* left ventricular, *PM* papillary muscles

development of FMR [11]. FMR has also been proposed to occur in LV dyssynchrony. In this instance, the mechanism is believed to be due to a combination of reduced closing force and discoordination of contraction of the papillary muscles, which results in dynamic tethering of the leaflets [12].

Mitral Valve Anatomy and the Underlying Mechanism of Functional Mitral Regurgitation

To understand the underlying pathophysiology associated with FMR and to diagnose FMR require an understanding of the normal mitral valve anatomy. This is important as treatment approaches are different in patients with primary versus FMR. In the case of primary mitral regurgitation, treatment strategies will target the mitral valve as opposed to FMR where the target strategies will predominantly be focused on the left ventricle. The anatomic structure of the mitral valve apparatus is complex and is composed of several components working in synchrony to open during diastole and close in systole effectively within the high-pressure systemic environment (see also Chap. 7). Essentially, the mitral valve is comprised of: (1) annulus, (2) leaflets, (3) chordae tendinae, and (4) papillary muscles. These will now be individually examined in the context of FMR.

Mitral Annulus

The mitral annulus is the anatomical poorly defined junctional zone, which separates the left atrium and left ventricle, to which the mitral leaflets are attached. It is oval in shape with the intercommissural diameter being larger than the anteroposterior diameter (Fig. 10.2). There is evidence that the mitral annulus is not simply a rigid fibrous ring but is pliable, and has been shown to undergo dynamic changes in shape and area throughout the cardiac cycle. Three-dimensional echocardiography (3DE) has revealed that the mitral annulus adopts a non-planar saddle-shape (Fig. 10.3). The anterior portion of the mitral annulus, which continuous with the aortic annulus, serves as the highest point (most atrial) of the mitral annulus and is more fibrous compared to the rest of the annulus, thus less prone to dilatation. On the other hand, the posterior annulus, which comprises of the remaining two-thirds of the annulus is more muscular, includes the low points of the saddle close to the lateral and medial commissures which are more loosely anchored to the surrounding tissue, hence able to move more freely with myocardial contraction and relaxation [13]. The posterior annulus is often the part of the mitral annulus, which dilates with significant mitral regurgitation, and is more prone to calcification [14]. The dynamic pliable nature of the mitral annu-

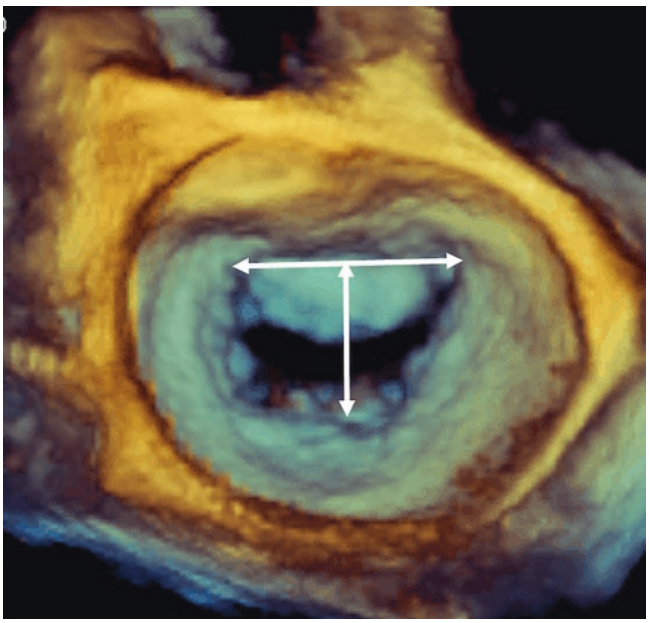

Fig. 10.2 3DE image of the mitral valve as viewed from the left atrium showing the D shape of the mitral annulus. The intercommissural diameter (horizontal arrow) is larger than the anteroposterior diameter (vertical arrow)

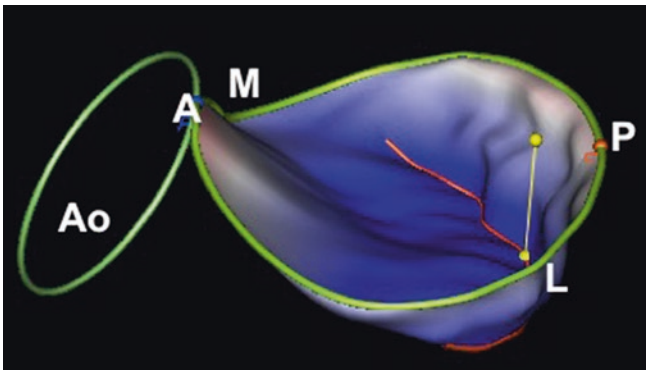

Fig. 10.3 3DE reconstruction of normal mitral valve annulus showing bimodal shape with high points (superiorly directed toward left atrium) located anterior-posterior orientation and low points located in medial-lateral orientation. *A* anterior, *Ao* aortic annulus, *L* lateral, *M* medial, *P* posterior

lus allows for systolic apical bending along a mediolateral commissure axis, and reciprocal systolic and diastolic changes in mitral annulus area [15–17]. Dynamic changes in the shape and area throughout the cardiac cycle have been shown to play an important role in maintaining the geometry of the mitral leaflets, aiding leaflet coaptation, reduce leaflet tissue stress and preventing unfavorable mitral leaflet remodeling [18–25]. Hence, morphological changes of the valve may potentially affect mechanical integrity of the total valve structure, resulting in abnormal leaflet closure and regurgitation of blood back into the left atrium. Interestingly, various

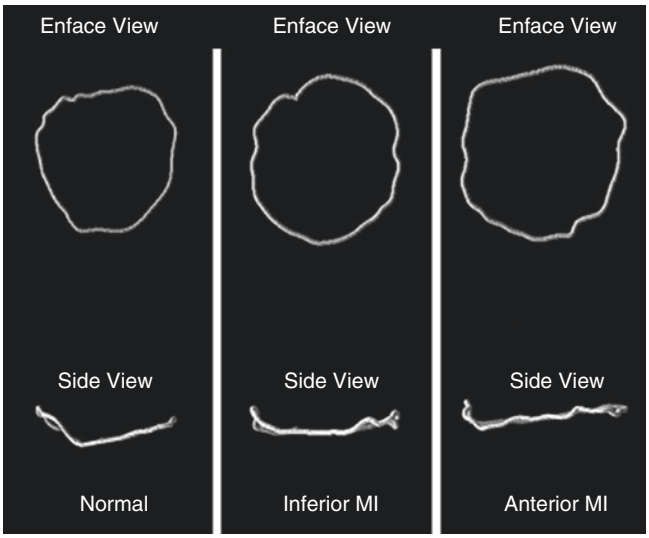

Fig. 10.4 Loss of saddle shape with infarction [33]. Adapted from Watanabe et al. Circulation 2005;112 9 Suppl:I458–I462

imaging modalities have quantified the average mitral annular area in healthy subjects to be approximately 10 cm^2 [26–31]. In pathological states such as in the case of dilatation of the LV, a significant increase in mitral annular area [26–28], decrease and delay of mitral annular area reduction during systole [28, 32] and flattening [28, 33] of its shape has been demonstrated [28, 32]. While mitral annular flattening has also been described in myxomatous valve disease, associated with more severe mitral regurgitation and chordal rupture, these are potentially though to be more likely related to increased out-of-plane stresses [18, 34]. Studies have demonstrated that the mitral annulus dilates and becomes flatter in response to development of FMR (Fig. 10.4) [35, 36].

Mitral Leaflets

The mitral valve comprises of two leaflets with variable commissural scallops to occlude medial and lateral gap, which lie within the ventricular inlet portion and have inherent differences in structure. The leaflets attach to the mitral annulus circumferentially with a minimum tissue length of 0.5–1 cm [37]. The anterior leaflet is trapezoid- or dome-shaped and much broader, longer and thicker but is attached to only one third of the annular circumference as compared to the narrower crescentic posterior leaflet with a long circumferential base [13] and relatively short radial length, which extends the remaining two-thirds of the annular diameter. Even though the posterior mitral leaflet appears smaller compared to the anterior leaflet, it has a larger area i.e. approximately 5 vs. 3 cm^2 respectively. The predominant feature of the anterior leaflet is the fibrous continuity with the left and non-coronary cusps of

the aortic valve and with the interleaflet triangle between the aortic cusps that abuts onto the membranous septum [14]. It is also thicker and thus allows the leaflet to withstand a significantly higher tensile load without tissue disruption compared to the posterior leaflet which is thinner and more flexible [38, 39]. The anterior leaflet is divided into three arbitrary segments (scallops), A1, A2 and A3, which correspond to adjacent regions on the posterior leaflet, P1, P2 and P3 delineated by 2 clefts (partial indentations in the leaflet which do not typically extend all the way through the leaflet). A1 and P1 being the most lateral segments, lie adjacent to the anterolateral commissure while A3 and P3 being the most medial, is adjacent to the posteromedial commissure. One other key point to note is that the nomenclature of the leaflets can be different based on whether the Carpentier numbering system (A1, A2, A3, P1, P2, P3; defined by where P1, P2, and P3, co-apt with the anterior leaflet) or the ASE/SCA anatomic nomenclature system (where there is a random division of the anterior leaflet into thirds; A1, the lateral third of the anterior leaflet; A2, the middle third of the anterior leaflet; A3, the medial third of anterior leaflet; P1, lateral scallop of posterior leaflet; P2, middle scallop of posterior leaflet; P3 medial scallop of posterior leaflet) is used [40, 41]. The commissural portions remain as the anterolateral commissure and posteromedial commissure in both nomenclature systems. Each of the leaflets can be characterized into three zones (basal, clear and rough zones), from their attachment point at the annulus to the free edge of the leaflet. The basal zone arises where the leaflet connects to the atrioventricular junction, followed by the thin, translucent central portion (body of the leaflet) known as the clear zone which then transitions into the rough zone, a hydrophilic protein rich zone measuring approximately 1 cm which incorporates the thicker free edge of the leaflets, and where chordal attachment, coaptation (i.e. where the leaflets meet) and apposition (overlap of the leaflet free edge) of the leaflets occur. Some redundant leaflet tissue is critically important for adequate leaflet apposition and tight leaflet coaptation while the irregular surface of the rough zone helps to maintain and ensure a seal during leaflet coaptation. A minimum leaflet to mitral annular area ratio of 1.5–2 has been shown to be necessary to prevent significant mitral regurgitation [27, 37]. In the case of FMR, dilatation of the left ventricle and thus the annulus significantly reduces the minimum leaflet to mitral annular ratio. Interestingly, physiologic or pathologic-induced leaflet stress can induce mitral leaflet adaptation as evidenced by the wide range of total leaflet area seen in various cardiac pathologies. Recently, 3DE have been used to provide valuable insight into the potential of the mitral leaflets to adapt i.e. mitral valve leaflets may be elongated in response to the stress imposed by increased tethering caused by dilated cardiomyopathy or inferior myocardial infarction [27, 42, 43]. However, the underlying cellular mechanisms underpinning the adaptive changes seen in the mitral leaflets are still not well understood. One study demonstrated that in patients with FMR and symmetrical tethering, mitral leaflet coaptation decreases proportionally to the bilateral papillary muscle displacement, despite the presence of increased total leaflet area. This study also found that the coaptation area was a strong determinant of mitral regurgitation severity [27].

Chordae Tendineae

The chordae tendinae are fan-shaped fibrous chords running from the papillary muscles and attaching into the anterior and posterior leaflets in an organized manner which serve to dampen the papillary muscle-leaflet force transmission [44]. Chordae arising from the anterolateral papillary muscle attach to A1, anterolateral commissure, P1, and the lateral half of P2 and A2. Chordae arising from the posteromedial papillary muscle attach to, A3, posteromedial commissure, P3, and medial half of P2, and A2. The chordae can also be categorized into three types based on their area of attachments on the leaflets: primary chordae attach to the free edge of both leaflets within the rough zone; secondary chordae attach to the ventricular surface in the region of the rough zone in the case of the anterior leaflet and throughout the posterior leaflet body [45], and tertiary chordae found associated with in the basal zone posterior leaflet only. Primary chordae are thinner and shorter (average length approximately 1–2 mm) compared to secondary chordae (average length approximately 20 mm), have limited extensibility [46] and serve predominantly to prevent leaflet edge eversion [45, 47–49]. Secondary chordae being thicker than primary chordae, are also more extensible than the primary chordae [46]. Of particular note are a pair of prominent thick secondary chordae thought to be the strongest chordae, termed strut chordae, arising from the tip of each papillary muscle and inserting into the ventricular aspect of the anterior leaflet [14]. Typically one arises from the anterior papillary muscle and attaches to A1/A2 area of the anterior leaflet; one arises from the posterior papillary muscle and attaches to the A2/A3 portion of the anterior leaflet although additional strut chords, including to the posterior leaflet have been described. Similar to mitral leaflets, the chordae tendinae also have the ability to adapt to altered loading conditions [47]. Interestingly, pathologic apical leaflet tethering can be relieved and mitral leaflet coaptation restored in patients with functional/ischemic mitral regurgitation, by cutting selected secondary chordae without deleterious effects on LV function [50–52].

Papillary Muscles

In a normal mitral valve, there are usually two associated papillary muscles named, based on their position, i.e. anterolateral and posteromedial papillary muscles. These are essentially large trabeculae originating along the mid to apical segments of the left ventricular wall in a plane posterior to the inter-commissural plane in diastole and usually only have one head (although double, triple or multiple heads are also possible variants) [53]. More specifically, the anterolateral papillary muscle is usually seen to attach at the border of the anterolateral (lateral) free wall of the LV and the posteromedial over the inferior wall of the LV at the junction of the inferior left ventricular free wall and the muscular ventricular septum with both papillary muscles extending into the upper third of the ventricular cavity below the commissural tissue. In terms of blood supply, there is common dual supply to the anterolateral papillary muscle, i.e. the first obtuse marginal arising from the left circumflex and the first diagonal arising from the anterior descending artery as opposed to the posteromedial which is only supplied by a single artery (usually from the right coronary artery or the third obtuse marginal of the left circumflex). The papillary muscle contraction maintains the systolic spatial relationship between the mitral annulus and the papillary muscle heads as the myocardium contracts, thereby preventing leaflet prolapse [54–56]. The papillary muscle head positions and relative distance to each other keep both leaflets under outwardly-directed tension and therefore posteriorly restrained to prevent anterior motion. Any damage sustained by the papillary muscles such as a localized area of infarction may result in remodeling and subsequent tethering of the leaflets by outward displacement of the myocardium underlying the papillary muscle (Fig. 10.5). On the other hand, global left ventricular dilatation and increased LV sphericity potentially restricts leaflet closure by displacing the papillary muscles potentially increasing the distance from the papillary muscle

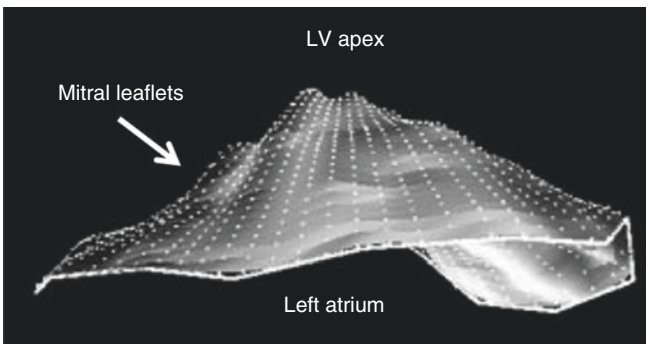

Fig. 10.5 Tethered leaflets (white arrow) with apically displaced coaptation line and increased tenting volume in a patient with functional mitral regurgitation

to the leaflet and thus causing tethering [57]. However, ischemic and/or systolic papillary muscle dysfunction itself does not seem to contribute to FMR on top of the contribution of papillary muscle displacement. This is evidenced by results from a sheep model of chronic ischemic mitral regurgitation which demonstrated that papillary ischemia as measured by decreased strain rate correlated with diminished tethering distances and reduced mitral regurgitation [58]. Similarly, in humans, there is also some evidence that papillary muscle dysfunction, as measured by longitudinal systolic strain, actually reduces mitral regurgitation observed after inferior myocardial infarction highlighting that impairment of papillary muscle contraction presumably reduces tension on the chordae and paradoxically compensates for the tethering forces exerted by papillary muscle misalignment and/or left ventricular dilatation. These observations support the hypothesis that geometric papillary muscle displacement, and not necessarily systolic function, is the key factor in determining functional mitral regurgitation.

3DE has been applied to measure quantitative mitral valve geometric parameters such as mitral annular area and shape, leaflet area, tenting volume (volume underneath leaflets to mitral annular plane in systole) (Fig. 10.6, left panel), and tethering distances (distance from papillary muscle tips to mitral valve trigone) (Fig. 10.6, right panel). These quantitative measures of mitral valve geometry can be valuable tools to demonstrate mechanism and clinical outcome associations [59].

Assessment of Severity of Functional Mitral Regurgitation

There have been a number of methods used to assess the severity of FMR. Direct surgical measurements have been proposed as the gold standard for the assessment of the severity of FMR. However, direct surgical measurements are impractical in the clinical setting as they can only be performed on the arrested heart and do not accurate reflect physiological conditions. There are also a number of non-invasive methods such as echocardiography, cardiac computed tomography [60, 61] and cardiac magnetic resonance [62, 63] that have been used successfully to assess and characterize FMR but none have been identified as the gold standard. Hence a true gold standard technique for assessment of FMR is presently still lacking [64, 65]. Of all these imaging modalities, echocardiography is recommended as the first line investigation. Echocardiography is more readily available and relatively cheaper compared to the other imaging modalities. It has the ability to provide live images of the beating heart, allowing for dynamic quantification from moving images, quantitative analysis on frozen frames throughout the cardiac cycle and,

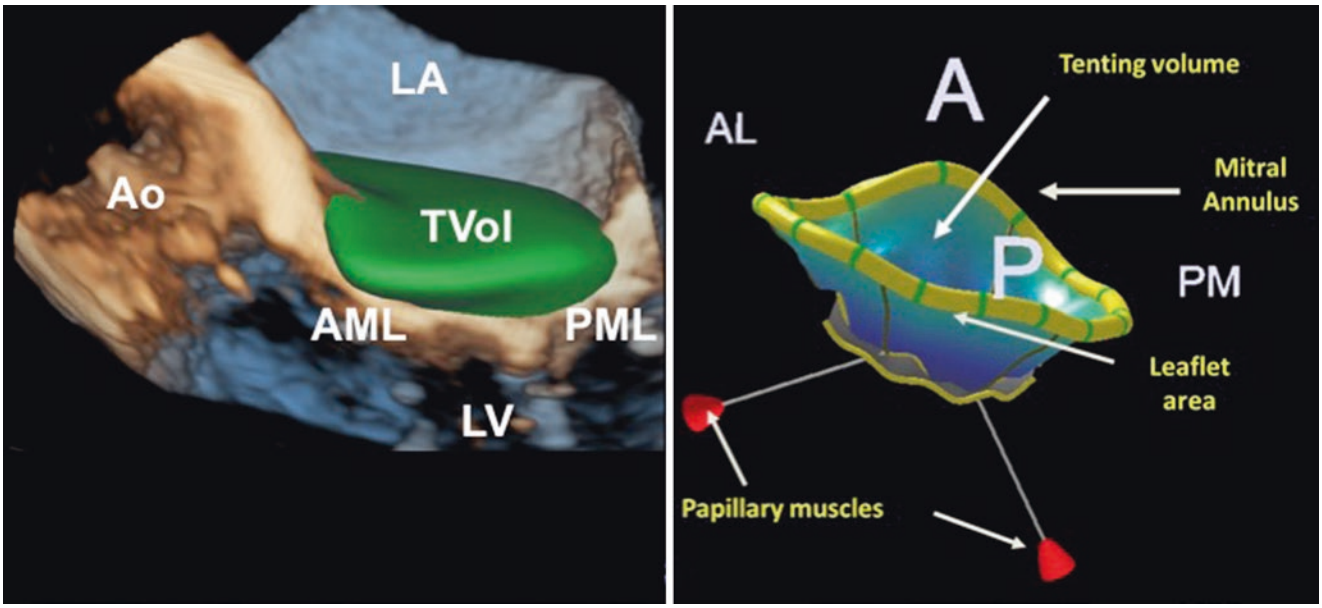

Fig. 10.6 Mitral valve geometry in functional mitral regurgitation. *Left panel*, the tenting volume is the space between the atrial surface of mitral valve leaflets and the mitral annulus. *Right panel*, quantitative measures including tenting volume, mitral annulus and leaflet area can be obtained from 3DE dataset of mitral valve using commercially available software package (Mitral Valve Navigator in QLab 10, Philips Medical Systems, Andover, USA). *A* anterior, *AML* anterior mitral leaflet, *AL* anterolateral, *Ao* aortic root, *LA* left atrium, *LV* left ventricle, *P* posterior, *PM* posteromedial, *TVol* tenting volume

measurements which are performed under more physiologic loading condition. Furthermore echocardiography, which does not utilise ionising radiation and is more readily available, can also be used to perform serial assessments allowing for characterization of progressive morphological changes induced by disease particularly those to the ventricle and allows for better understanding of the temporal trends of the underlying disease process [13, 66, 67]. Current guidelines recommend that asymptomatic patients with significant mitral regurgitation undergo serial echocardiography every 6–12 months to assess LV size and systolic function as this information is important for informing optimal timing for surgery intervention (Class I) [68]. One key point to note is that FMR occurs due to a complex interplay of geometric and contractile abnormalities, its severity can vary during the cardiac cycle and with ventricular loading conditions hence assessment of FMR can be very challenging [69]. FMR must always be interpreted in the context of loading conditions. Ambient preload and afterload conditions such as patient's volume status, systemic blood pressure, and medications may affect the observed degree of mitral regurgitation. Hence the blood pressure and medications at the time of assessment should always be considered and factored in the assessment of the severity of regurgitation.

Echocardiographic Assessment of Severity Functional Mitral Regurgitation

The echocardiographic assessment of FMR can be categorised into the assessment of the morphology of the mitral valve leaflets and the associated structures (in order to help delineate the aetiology of the mitral regurgitation) and severity of valve disease, which is essential for management planning [66, 67, 70, 71]. Assessment of mitral valve morphology is important as it also allows for determination of clinical or haemodynamic consequences. The presence of the "seagull" sign due to chordal tethering and kinking of the anterior leaflet in its mid-belly can be helpful in identifying FMR. The tethering of the leaflets can potentially also be quantified by the measures of tenting height (also named coaptation height or coaptation depth). The tenting height represents the distance from the annulus plane of the mitral valve to the leaflet coaptation point whereas the tenting area and volume represent more global measures of tethering of the leaflets [72–75] (Fig. 10.7, Video 10.1). The tethering angles can also be used to quantify individual leaflet tethering [74]. In terms of the tethering angles, the anterior leaflet can be characterised by two angles, a proximal tethering angle and a distal tethering angle, as being more prone to tethering forces can bend a wider range of compared to the posterior leaflet.

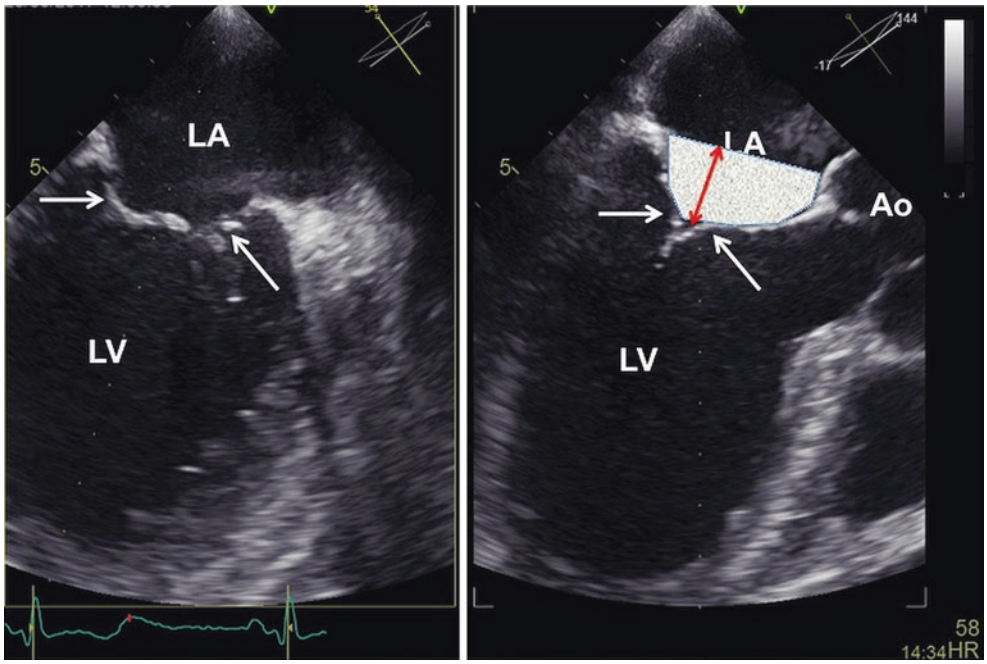

Fig. 10.7 Biplane image of dilated left ventricle showing tethering (white arrows) of the mitral leaflets resulting in incomplete coaptation. Tethering is the fundamental mechanism of functional mitral regurgitation (Video 10.1). The gray area is the tenting area and the coaptation depth is shown by the double head red arrow. *Ao* aortic root, *LA* left atrium, *LV* left ventricle

Current American College of Cardiology/American Heart Association guidelines recommend that two-dimensional and Doppler echocardiography be used to assess all patients with suspected mitral regurgitation to confirm its presence and determine its severity (according to the Functional Class), i.e. assessment of severity should based on a combination of echocardiographic and symptomatic parameters, with stages of "at risk" to "progressive" to "asymptomatic severe" to "symptomatic severe" [68]. Quantitative analysis is also an integral part of the assessment and provides objective evidence for the classification of the degree of severity of the mitral regurgitation. Current guidelines also recommend the integration of a number of specific, supportive, and quantitative features including cardiac chamber size and volume, regurgitant jet size by color Doppler, regurgitant jet density by continuous-wave Doppler, and pulmonary vein and mitral valve inflow by pulse-wave Doppler in classifying the severity of the mitral regurgitation [1, 65]. Additionally, Doppler echocardiography allow for quantitative measurement of mitral regurgitation, including the regurgitant volume and the regurgitant orifice area. In addition to semi-quantitative and quantitative Doppler techniques, it is important to integrate supportive and complementary data into the overall severity grading. Pulmonary venous flow reversal is specific for severe mitral regurgitation although of lower sensitivity. Chamber enlargement (left atrium and LV), dense continuous wave mitral regurgitation Doppler profile, and elevated E wave peak velocity >1.2 m/s are all suggestive of severe mitral regurgitation [76].

However, defining FMR and quantification of the severity of FMR can be very challenging using standard two-dimensional echocardiographic techniques due to the considerable clinical heterogeneity seen. Furthermore, the geometric distortions underlying FMR result in failure of the coaptation along the closure line of the valve in a variable manner such that the regurgitant orifice is non-circular but elliptical or slit-like. Additionally, mitral regurgitation may be complex with several separate regurgitant orifices along the closure line. This potentially impacts on the accuracy of standard recommended two-dimensional measures used in the quantification of the severity of mitral regurgitation, particularly measures dependent on flow or flow quantification, due to the complex spatial and dynamic patterns of flow across the mitral valve. While these quantitative techniques can be accurate and reproducible in single centers [77, 78], there can be significant interobserver variability among centers [79]. The application of 3DE has allowed some of the geometric limitations seen with two-dimensional echocardiography to potentially be overcome.

Assessment of Effective Regurgitant Orifice Area and Regurgitant Volume

The effective regurgitant orifice area and regurgitant volume can be assessed using a number of approaches. Evaluation of both the effective regurgitant orifice area and regurgitant volume are currently also recommended in current guidelines in

the assessment of mitral regurgitation [1, 65]. However, all methods outlined below, if performed with two-dimensional echocardiography imaging have limitations and are often inaccurate due to the multiple indirect measurements required, imprecise hemodynamic assumptions frequently lead to inaccurate assessments [64, 78, 80, 81].

Vena Contracta

Given that the vena contracta area is also the effective orifice area, vena contracta width is an accepted direct assessment of the effective regurgitant orifice area. It is defined as the narrowest cross section of the regurgitant jet [65, 77, 82] and assumes that the regurgitant orifice is virtually circular. Measurements made from transesophageal echo images are more accurate than those made from transthoracic echo images [65]. Vena contracta width measurements appear to be less influenced by instrument settings compared to other quantitative techniques [65] and appear to be reasonably accurate indicators severity of mitral regurgition, regardless of the mitral regurgitation etiology and jet direction [76]. However, limitations of this method include the fact that small measurement errors can also result in the misclassification of MR severity. Furthermore, the exact shape and size of the regurgitant orifice is not accurately assessed nor factored into this measurement due to the limited scan plane orientation of two-dimensional echocardiography. Traditionally, the vena contracta is assessed in the parasternal long-axis view or apical three-chamber view and is measured as the diameter of the narrowest part of the regurgitant jet as it passes through the regurgitant orifice and is a reasonable estimate of severity [1]. However in the instance of an elliptical orifice, the extent of regurgitation may be underestimated or overestimated dependent on the view where the measurement is made [83].

3DE allows for direct visualization of the effective regurgitant orifice thus allowing direct planimetry of the vena contracta area. (Fig. 10.8, Video 10.2a Left and 10.2b Right) This is particularly relevant for patients with FMR, where the effective regurgitant orifice geometry is usually complex and asymmetric [84, 85] therefore measurements done using 3DE greatly improves the accuracy of the assessment of the effective regurgitant orifice area in this patient group. Using color Doppler 3DE image plane orientation can be adjusted to the true plane of the regurgitant orifice for direct quantification of the regurgitant area [83, 84, 86] (Fig. 10.9). Correlative studies with cardiac magnetic resonance have demonstrated a good correlation between regurgitant volume derived from effective regurgitant orifice measured by 3DE planimetry and that measured using velocity-encoded cardiac magnetic resonance imaging compared to two-dimensional echocardiography measures which consistently underestimated both effective regurgitant orifice area and regurgitant volume [69]. Additionally, the vena contracta area has also been shown to frequently not to be circular as assumed but asymmetric in the majority of patients and etiologies. (Fig. 10.10, Video 10.3) Nonetheless, a true

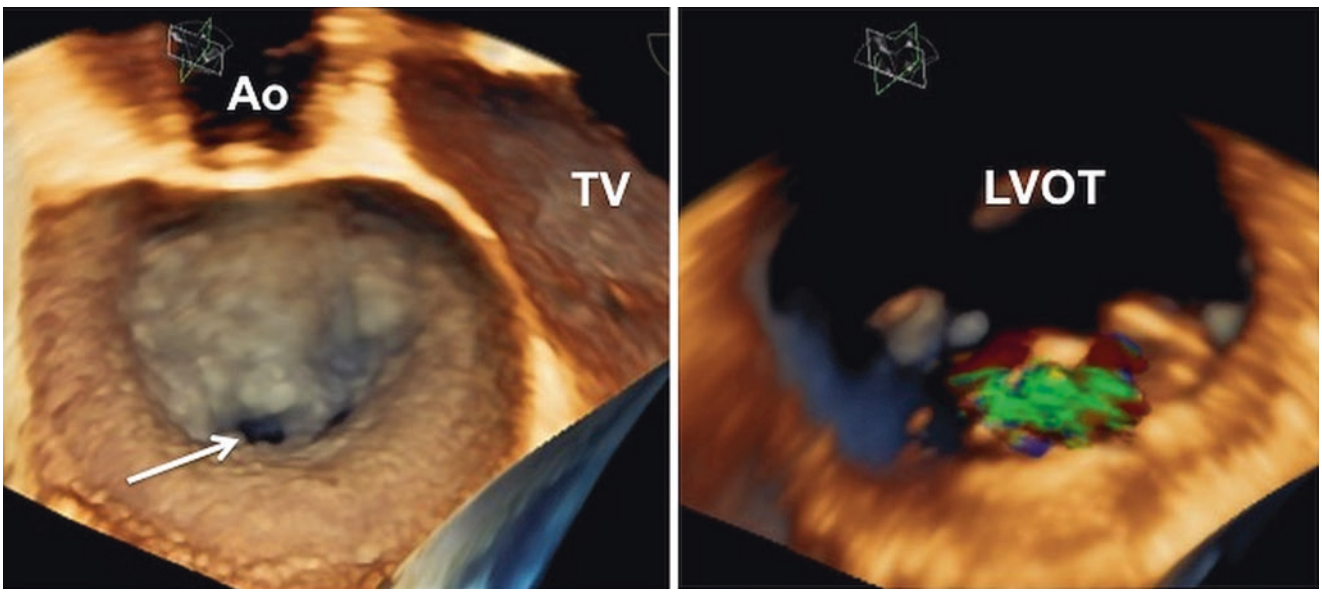

Fig. 10.8 Incomplete closure due to leaflet tethering. *Left panel*: transesophageal 3DE image of the mitral valve viewed from left atrium in a patient with functional mitral regurgitation. There is a visible gap along the coaptation line due to tethered mitral leaflets (white arrow, Video 10.2a Left). *Right panel*: Corresponding 3DE color Doppler image of the mitral valve seen from the left ventricular perspective showing origin of functional mitral regurgitation jet is through this gap (Video 10.2b Right). *Ao* aortic valve, *LVOT* left ventricular outflow tract, *TV* tricuspid valve

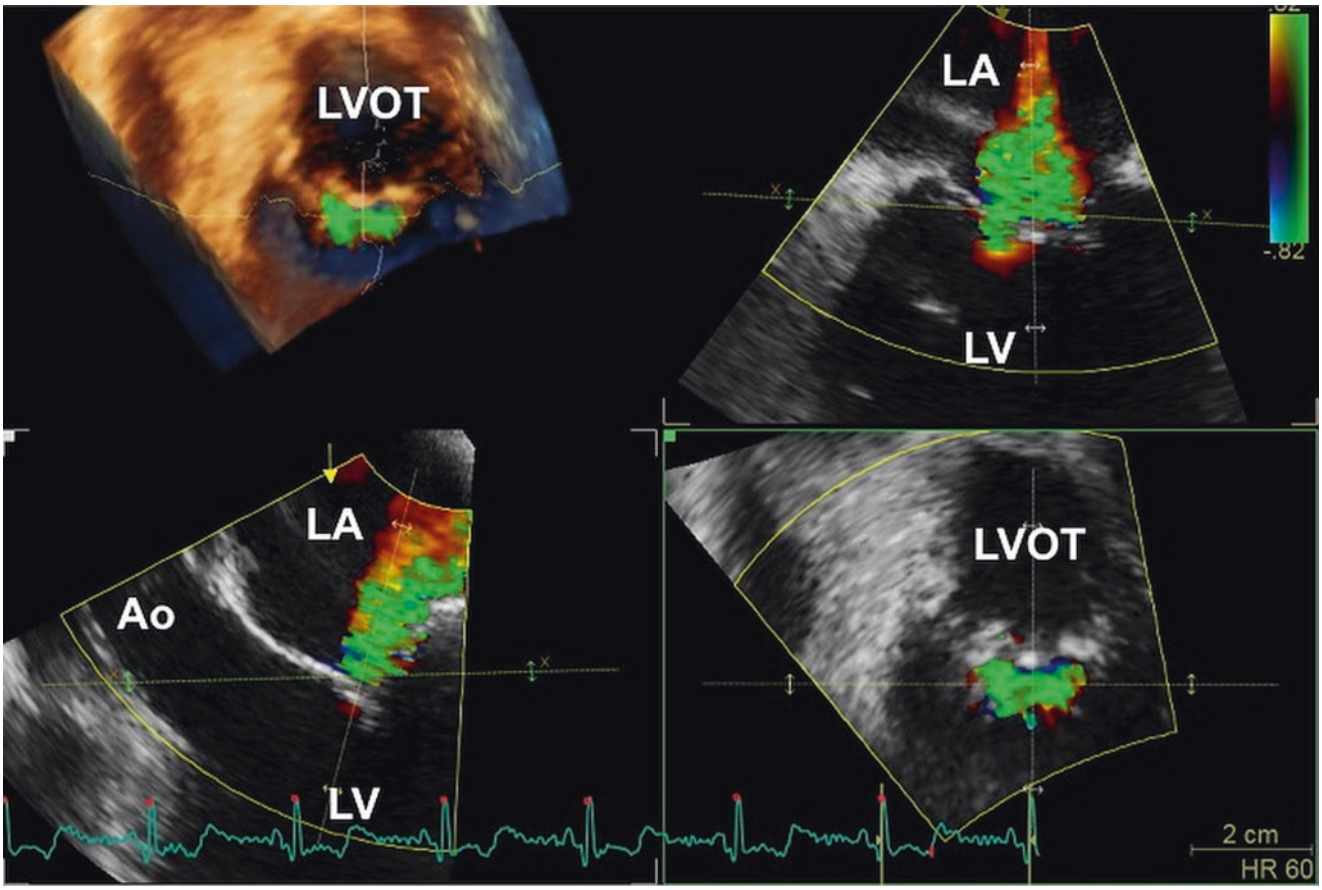

Fig. 10.9 Complexity of the geometry of the regurgitant orifice in functional mitral regurgitation. In most of the patients with functional mitral regurgitation, the valve leaks along part or the entire coaptation line as shown in the transesophageal 3DE color Doppler data set of the mitral valve seen *en face* from the ventricular perspective (*upper left panel*). This means that the shape of the regurgitant orifice is more oval or slit like than rounded, and measurement of a single diameter of the vena contracta may be misleading. Erroneously small if measured perpendicular to the coaptation line (*lower left panel*), or very large if measured along the coaptation line (*upper right panel*). A cut plane (green dotted line) positioned at the level of the narrowest part of the regurgitant orifice, and perpendicular to the direction of the jet, allows to visualize the actual vena contracta shape and size (*lower right panel*). *Ao* aortic valve, *LA* left atrium, *LV* left ventricle, *LVOT* left ventricular outflow area

validation study of 3DE measurements of effective regurgitant orifice area is lacking [83, 84, 87].

Proximal Isovelocity Surface Area

Calculation of effective regurgitant orifice area and regurgitant volumes can also be obtained by using Doppler techniques such as the proximal flow convergence method using color Doppler. The proximal isovelocity surface area (PISA) method provides a quantitative method for grading of mitral regurgitation. In this approach the following formula are used to calculate the effective regurgitant orifice area and regurgitant volume respectively.

$$\text{EROA} = 2\text{pR}^2 \times \text{Aliasing Velocity} \div \text{Peak Velocity of mitral regurgitation}$$

where R is the radius of the hemispheric PISA zone

$$\text{Regurgitant Volume} = \text{EROA} \times \text{TVI of the continuous wave Doppler profile of the mitral regurgitation}$$

The dynamic nature of FMR is also a major challenge to quantification using standard flow convergence methods utilizing the proximal isovelocity area (Video 10.4). Traditionally, the mid-systolic PISA coincident with the peak regurgitant velocity is used to estimate peak regurgitant flow rate and from that the maximal effective regurgitant orifice area and the regurgitant stroke volume. However, this approach is based on the assumption that the mid-systolic PISA is truly maximal (i.e. that the effective regurgitant orifice area is largest and mitral regurgitation the worst) [1]. In functional mitral regurgitation, the mid-systolic PISA is generally the smallest as there is improved coaptation due

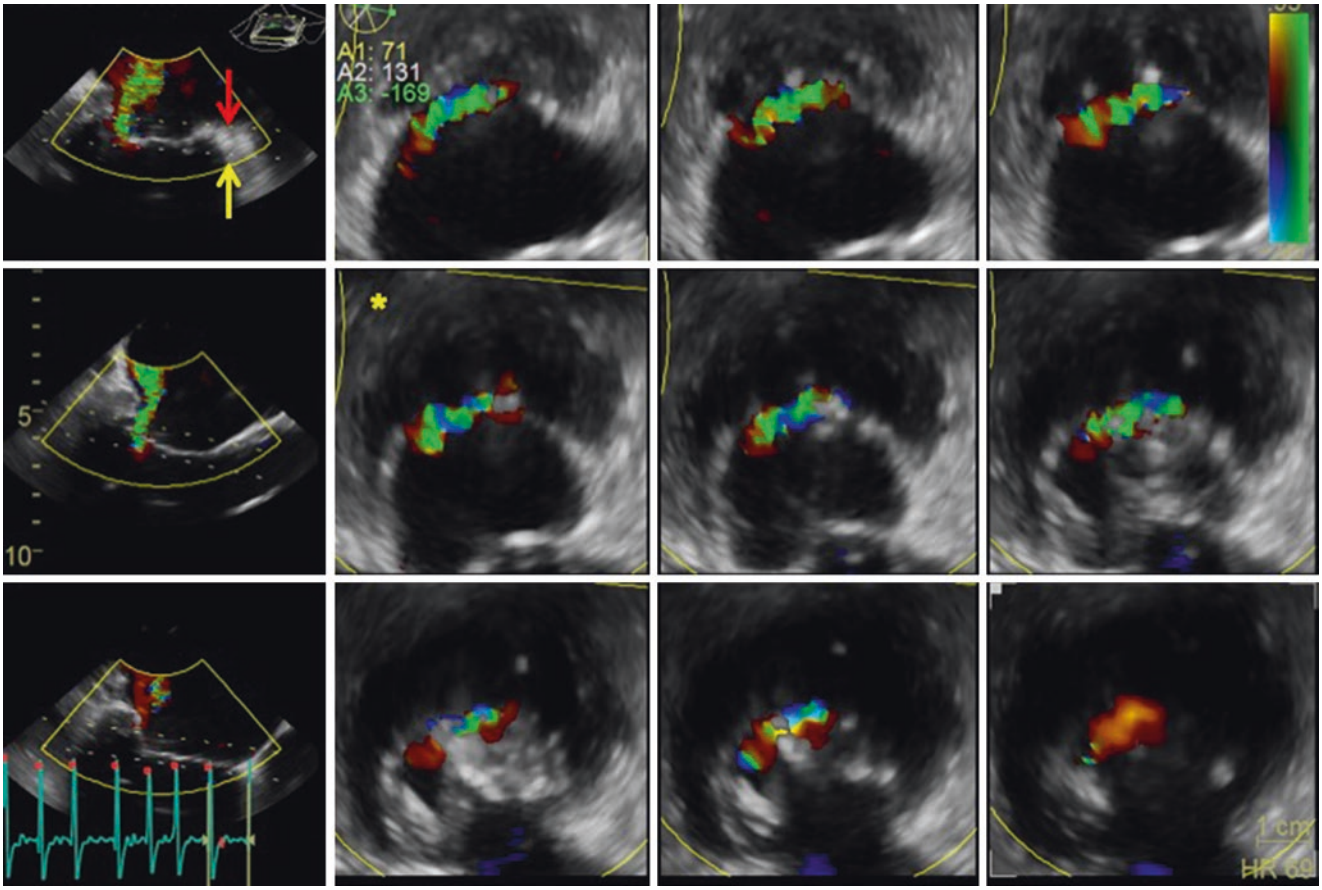

Fig. 10.10 Methodology to identify the vena contracta of the regurgitant mitral jet using transesophageal 3DE color Doppler. The 3DE color Doppler is displayed in multislice mode. The upper (yellow dotted line showed by the red arrow) and the lower (yellow dotted line showed by the yellow arrow) cut plane are positioned in order to include the proximal isovelocity area and the proximal part of the jet, perpendicular to the direction of the jet, in order to have multiple slice in the proximal part of the jet (Video 10.3). The smallest among the color Doppler area displayed in the multislice will be the true vena contracta and its area can be planimetered (yellow asterisk)

to maximal closing forces hence the effective regurgitant orifice is smaller. Hence the haemodynamic workload is underestimated if only a single mid-systolic point is used. Similarly, the effective regurgitant orifice area is likely to be overestimated if a maximal PISA in early or late systole is selected which does not coincide with the mid-systolic peak regurgitant velocity [69, 84]. Characterization of the PISAs in a population of patients with mitral regurgitation also revealed a heterogeneous spread of PISAs with the location and nature of the PISA dependent on the underlying geometry of the valve (Fig. 10.11). This study revealed that approximately 50% have a PISA away from the midpoint of the closure line, 35% have PISAs that are dominant in both the medial and lateral aspects of the closure line and relatively small in the centre, and approximately 25% have multiple separate PISAs suggesting that the standard two-dimensional echocardiography techniques do not provide an accurate estimate of the severity of regurgitation [88]. Another study which compared four different PISA methods against volumetric cardiac magnetic resonance as the gold standard highlighted that mid-systolic single time point estimates of PISA substantially underestimate the severity of FMR compared with cardiac magnetic resonance [88]. 3DE assessment of PISA shape has demonstrated that the hemispherical assumption is often not present-especially in functional mitral regurgitation where it is often hemielliptical (Fig. 10.12). Adoption of a hemisphere likely accounts for the underestimation of effective regurgitant orifice area in two-dimensional PISA methods of measuring effective regurgitant orifice area [76].

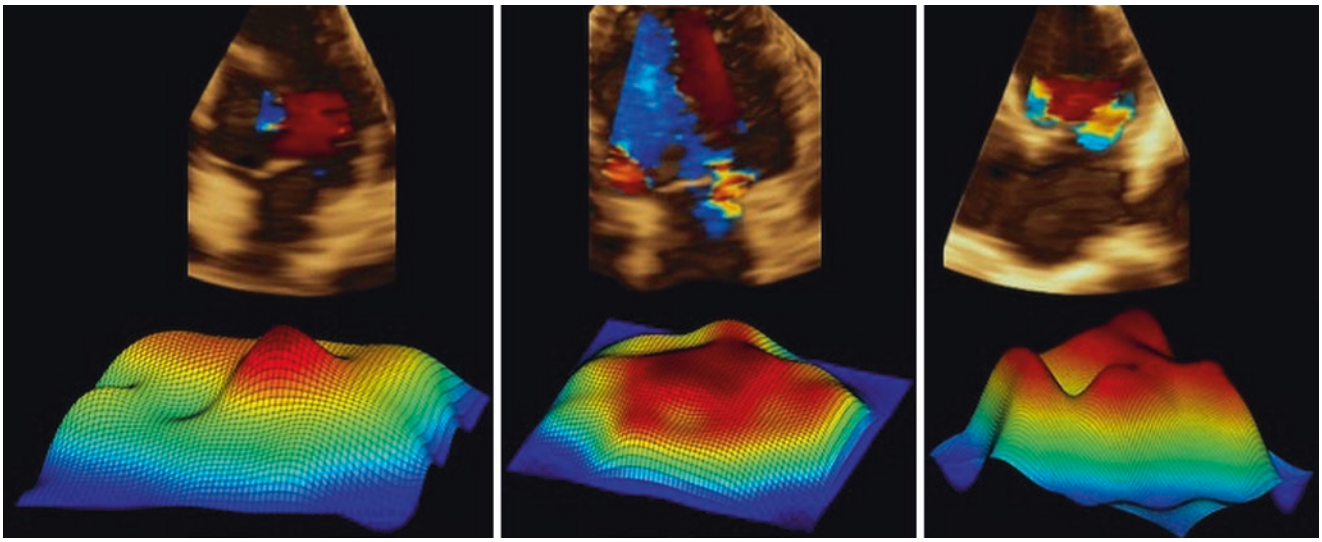

Fig. 10.11 3DE computerized reconstruction of the actual geometry of the proximal isovelocity surface are in three patients with various degrees and causes of functional mitral regurgitation. Actually, proximal isovelocity surface is almost never a hemisphere and calculations of its area based on a single diameter may be misleading

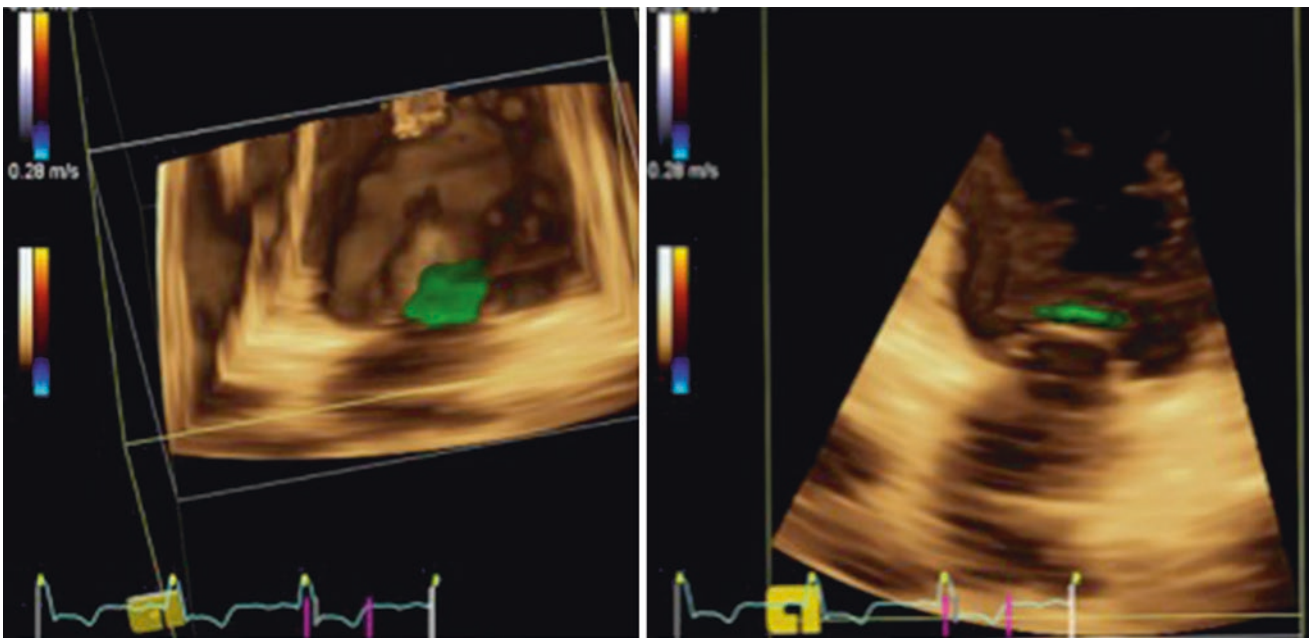

Fig. 10.12 3DE geometry of the actual proximal isovelocity surface area/volume in a patient with functional mitral regurgitation seen an face (*left panel*) and from a side (*right panel*)

Alternative Methods for Quantification of Mitral Regurgitant Volume

Another method to calculate the mitral regurgitant volume is the pulsed Doppler volumetric method, which determines the mitral regurgitant volume by subtracting the aortic forward stroke volume from the total stroke volume through the mitral annulus [1, 65]. This method requires two non-stenotic valves without significant aortic regurgitation.

Stress Echocardiography

Exercise stress echocardiography may also be useful in the assessment of FMR particularly in the context of determining clinical significance i.e. objective measure of exercise tolerance in a patient, worsening in the severity of mitral regurgitation, pulmonary pressure, and contractile reserve to exercise (Class IIa) [68]. Exercise may provoke hemodynamically significant mitral regurgitation in patients who

have a degree of exertional dyspnea is out of keeping with the extent of LV dysfunction or degree of regurgitation at rest and pulmonary edema without an obvious cause [89]. Furthermore, an exercise-induced increase in effective regurgitant orifice area of ≥13 mm^2 is associated with increased morbidity and mortality [90]. Dobutamine stress echo may also be useful to determine the extent of viable myocardium that might recover with revascularization, effectiveness of medical treatment, or possibly resynchronization but is not so useful in assessing the severity of FMR as it has direct effects on loading conditions [91].

References

1. Lancellotti P, Moura L, Pierard LA, Agricola E, Popescu BA, Tribouilloy C, et al. European Association of Echocardiography recommendations for the assessment of valvular regurgitation. Part 2: mitral and tricuspid regurgitation (native valve disease). Eur J Echocardiogr. 2010;11:307–32.
2. Nkomo VT, Gardin JM, Skelton TN, Gottdiener JS, Scott CG, Enriquez-Sarano M. Burden of valvular heart diseases: a population-based study. Lancet. 2006;368:1005–11.
3. Bursi F, Enriquez-Sarano M, Nkomo VT, Jacobsen SJ, Weston SA, Meverden RA, et al. Heart failure and death after myocardial infarction in the community: the emerging role of mitral regurgitation. Circulation. 2005;111:295–301.
4. Grigioni F, Detaint D, Avierinos JF, Scott C, Tajik J, Enriquez-Sarano M. Contribution of ischemic mitral regurgitation to congestive heart failure after myocardial infarction. J Am Coll Cardiol. 2005;45:260–7.
5. Grigioni F, Enriquez-Sarano M, Zehr KJ, Bailey KR, Tajik AJ. Ischemic mitral regurgitation: long-term outcome and prognostic implications with quantitative Doppler assessment. Circulation. 2001;103:1759–64.
6. Iung B, Baron G, Butchart EG, Delahaye F, Gohlke-Barwolf C, Levang OW, et al. A prospective survey of patients with valvular heart disease in Europe: The Euro Heart Survey on Valvular Heart Disease. Eur Heart J. 2003;24:1231–43.
7. Enriquez-Sarano M, Avierinos JF, Messika-Zeitoun D, Detaint D, Capps M, Nkomo V, et al. Quantitative determinants of the outcome of asymptomatic mitral regurgitation. N Engl J Med. 2005;352:875–83.
8. Rosenhek R, Rader F, Klaar U, Gabriel H, Krejc M, Kalbeck D, et al. Outcome of watchful waiting in asymptomatic severe mitral regurgitation. Circulation. 2006;113:2238–44.
9. Patel JB, Borgeson DD, Barnes ME, Rihal CS, Daly RC, Redfield MM. Mitral regurgitation in patients with advanced systolic heart failure. J Card Fail. 2004;10:285–91.
10. Blondheim DS, Jacobs LE, Kotler MN, Costacurta GA, Parry WR. Dilated cardiomyopathy with mitral regurgitation: decreased survival despite a low frequency of left ventricular thrombus. Am Heart J. 1991;122:763–71.
11. Levine RA, Hagege AA, Judge DP, Padala M, Dal-Bianco JP, Aikawa E, et al. Mitral valve disease--morphology and mechanisms. Nat Rev Cardiol. 2015;12:689–710.
12. Kanzaki H, Bazaz R, Schwartzman D, Dohi K, Sade LE, Gorcsan J 3rd. A mechanism for immediate reduction in mitral regurgitation after cardiac resynchronization therapy: insights from mechanical activation strain mapping. J Am Coll Cardiol. 2004;44:1619–25.
13. Dal-Bianco JP, Levine RA. Anatomy of the mitral valve apparatus: role of 2D and 3D echocardiography. Cardiol Clin. 2013;31:151–64.
14. McCarthy KP, Ring L, Rana BS. Anatomy of the mitral valve: understanding the mitral valve complex in mitral regurgitation. Eur J Echocardiogr. 2010;11:i3–9.
15. Hamdan A, Guetta V, Konen E, Goitein O, Segev A, Raanani E, et al. Deformation dynamics and mechanical properties of the aortic annulus by 4-dimensional computed tomography: insights into the functional anatomy of the aortic valve complex and implications for transcatheter aortic valve therapy. J Am Coll Cardiol. 2012;59:119–27.
16. Lansac E, Lim KH, Shomura Y, Goetz WA, Lim HS, Rice NT, et al. Dynamic balance of the aortomitral junction. J Thorac Cardiovasc Surg. 2002;123:911–8.
17. Veronesi F, Corsi C, Sugeng L, Caiani EG, Weinert L, Mor-Avi V, et al. Quantification of mitral apparatus dynamics in functional and ischemic mitral regurgitation using real-time 3-dimensional echocardiography. J Am Soc Echocardiogr. 2008;21:347–54.
18. Jensen MO, Hagege AA, Otsuji Y, Levine RA, Leducq Transatlantic MN. The unsaddled annulus: biomechanical culprit in mitral valve prolapse? Circulation. 2013;127:766–8.
19. Jensen MO, Jensen H, Levine RA, Yoganathan AP, Andersen NT, Nygaard H, et al. Saddle-shaped mitral valve annuloplasty rings improve leaflet coaptation geometry. J Thorac Cardiovasc Surg. 2011;142:697–703.
20. Jensen MO, Jensen H, Smerup M, Levine RA, Yoganathan AP, Nygaard H, et al. Saddle-shaped mitral valve annuloplasty rings experience lower forces compared with flat rings. Circulation. 2008;118:S250–5.
21. Jimenez JH, Liou SW, Padala M, He Z, Sacks M, Gorman RC, et al. A saddle-shaped annulus reduces systolic strain on the central region of the mitral valve anterior leaflet. J Thorac Cardiovasc Surg. 2007;134:1562–8.
22. Kunzelman KS, Reimink MS, Cochran RP. Annular dilatation increases stress in the mitral valve and delays coaptation: a finite element computer model. Cardiovasc Surg. 1997;5:427–34.
23. Padala M, Hutchison RA, Croft LR, Jimenez JH, Gorman RC, Gorman JH 3rd, et al. Saddle shape of the mitral annulus reduces systolic strains on the P2 segment of the posterior mitral leaflet. Ann Thorac Surg. 2009;88:1499–504.
24. Reimink MS, Kunzelman KS, Verrier ED, Cochran RP. The effect of anterior chordal replacement on mitral valve function and stresses. A finite element study. ASAIO J. 1995; 41:M754–62.
25. Salgo IS, Gorman JH 3rd, Gorman RC, Jackson BM, Bowen FW, Plappert T, et al. Effect of annular shape on leaflet curvature in reducing mitral leaflet stress. Circulation. 2002;106:711–7.
26. Alkadhi H, Desbiolles L, Stolzmann P, Leschka S, Scheffel H, Plass A, et al. Mitral annular shape, size, and motion in normals and in patients with cardiomyopathy: evaluation with computed tomography. Invest Radiol. 2009;44:218–25.
27. Chaput M, Handschumacher MD, Tournoux F, Hua L, Guerrero JL, Vlahakes GJ, et al. Mitral leaflet adaptation to ventricular remodeling: occurrence and adequacy in patients with functional mitral regurgitation. Circulation. 2008;118:845–52.
28. Flachskampf FA, Chandra S, Gaddipatti A, Levine RA, Weyman AE, Ameling W, et al. Analysis of shape and motion of the mitral annulus in subjects with and without cardiomyopathy by echocardiographic 3-dimensional reconstruction. J Am Soc Echocardiogr. 2000;13:277–87.
29. Maffessanti F, Gripari P, Pontone G, Andreini D, Bertella E, Mushtaq S, et al. Three-dimensional dynamic assessment of tricuspid and mitral annuli using cardiovascular magnetic resonance. Eur Heart J Cardiovasc Imaging. 2013;14:986–95.
30. Ormiston JA, Shah PM, Tei C, Wong M. Size and motion of the mitral valve annulus in man. I. A two-dimensional echocardiographic method and findings in normal subjects. Circulation. 1981;64:113–20.

31. Veronesi F, Corsi C, Sugeng L, Mor-Avi V, Caiani EG, Weinert L, et al. A study of functional anatomy of aortic-mitral valve coupling using 3D matrix transesophageal echocardiography. Circ Cardiovasc Imaging. 2009;2:24–31.
32. Daimon M, Saracino G, Fukuda S, Koyama Y, Kwan J, Song JM, et al. Dynamic change of mitral annular geometry and motion in ischemic mitral regurgitation assessed by a computerized 3D echo method. Echocardiography. 2010;27:1069–77.
33. Watanabe N, Ogasawara Y, Yamaura Y, Wada N, Kawamoto T, Toyota E, et al. Mitral annulus flattens in ischemic mitral regurgitation: geometric differences between inferior and anterior myocardial infarction: a real-time 3-dimensional echocardiographic study. Circulation. 2005;112:I458–62.
34. Lee AP, Hsiung MC, Salgo IS, Fang F, Xie JM, Zhang YC, et al. Quantitative analysis of mitral valve morphology in mitral valve prolapse with real-time 3-dimensional echocardiography: importance of annular saddle shape in the pathogenesis of mitral regurgitation. Circulation. 2013;127:832–41.
35. Watanabe N, Ogasawara Y, Yamaura Y, Kawamoto T, Akasaka T, Yoshida K. Geometric deformity of the mitral annulus in patients with ischemic mitral regurgitation: a real-time three-dimensional echocardiographic study. J Heart Valve Dis. 2005;14:447–52.
36. Kwan J, Qin JX, Popovic ZB, Agler DA, Thomas JD, Shiota T. Geometric changes of mitral annulus assessed by real-time 3-dimensional echocardiography: becoming enlarged and less nonplanar in the anteroposterior direction during systole in proportion to global left ventricular systolic function. J Am Soc Echocardiogr. 2004;17:1179–84.
37. Chiechi MA, Lees WM, Thompson R. Functional anatomy of the normal mitral valve. J Thorac Surg. 1956;32:378–98.
38. Kunzelman KS, Cochran RP, Chuong C, Ring WS, Verrier ED, Eberhart RD. Finite element analysis of the mitral valve. J Heart Valve Dis. 1993;2:326–40.
39. Kunzelman KS, Cochran RP, Murphree SS, Ring WS, Verrier ED, Eberhart RC. Differential collagen distribution in the mitral valve and its influence on biomechanical behaviour. J Heart Valve Dis. 1993;2:236–44.
40. Carpentier AF, Lessana A, Relland JY, Belli E, Mihaileanu S, Berrebi AJ, et al. The "physio-ring": an advanced concept in mitral valve annuloplasty. Ann Thorac Surg. 1995;60:1177–85; discussion 85–6.
41. Shanewise JS, Cheung AT, Aronson S, Stewart WJ, Weiss RL, Mark JB, et al. ASE/SCA guidelines for performing a comprehensive intraoperative multiplane transesophageal echocardiography examination: recommendations of the American Society of Echocardiography Council for Intraoperative Echocardiography and the Society of Cardiovascular Anesthesiologists Task Force for Certification in Perioperative Transesophageal Echocardiography. J Am Soc Echocardiogr. 1999;12:884–900.
42. Chaput M, Handschumacher MD, Guerrero JL, Holmvang G, Dal-Bianco JP, Sullivan S, et al. Mitral leaflet adaptation to ventricular remodeling: prospective changes in a model of ischemic mitral regurgitation. Circulation. 2009;120:S99–103.
43. Dal-Bianco JP, Levine RA. The mitral valve is an actively adapting tissue: new imaging evidence. Eur Heart J Cardiovasc Imaging. 2015;16:286–7.
44. Millington-Sanders C, Meir A, Lawrence L, Stolinski C. Structure of chordae tendineae in the left ventricle of the human heart. J Anat. 1998;192(Pt 4):573–81.
45. Degandt AA, Weber PA, Saber HA, Duran CM. Mitral valve basal chordae: comparative anatomy and terminology. Ann Thorac Surg. 2007;84:1250–5.
46. Liao J, Vesely I. A structural basis for the size-related mechanical properties of mitral valve chordae tendineae. J Biomech. 2003;36:1125–33.
47. Dal-Bianco JP, Aikawa E, Bischoff J, Guerrero JL, Handschumacher MD, Sullivan S, et al. Active adaptation of the tethered mitral valve: insights into a compensatory mechanism for functional mitral regurgitation. Circulation. 2009;120:334–42.
48. Lam JH, Ranganathan N, Wigle ED, Silver MD. Morphology of the human mitral valve. I. Chordae tendineae: a new classification. Circulation. 1970;41:449–58.
49. Obadia JF, Casali C, Chassignolle JF, Janier M. Mitral subvalvular apparatus: different functions of primary and secondary chordae. Circulation. 1997;96:3124–8.
50. Messas E, Guerrero JL, Handschumacher MD, Conrad C, Chow CM, Sullivan S, et al. Chordal cutting: a new therapeutic approach for ischemic mitral regurgitation. Circulation. 2001;104:1958–63.
51. Messas E, Pouzet B, Touchot B, Guerrero JL, Vlahakes GJ, Desnos M, et al. Efficacy of chordal cutting to relieve chronic persistent ischemic mitral regurgitation. Circulation. 2003;108(Suppl 1):II111–5.
52. Messas E, Yosefy C, Chaput M, Guerrero JL, Sullivan S, Menasche P, et al. Chordal cutting does not adversely affect left ventricle contractile function. Circulation. 2006;114:I524–8.
53. Rusted IE, Scheifley CH, Edwards JE. Studies of the mitral valve. I. Anatomic features of the normal mitral valve and associated structures. Circulation. 1952;6:825–31.
54. Gorman JH 3rd, Gupta KB, Streicher JT, Gorman RC, Jackson BM, Ratcliffe MB, et al. Dynamic three-dimensional imaging of the mitral valve and left ventricle by rapid sonomicrometry array localization. J Thorac Cardiovasc Surg. 1996;112:712–26.
55. Joudinaud TM, Kegel CL, Flecher EM, Weber PA, Lansac E, Hvass U, et al. The papillary muscles as shock absorbers of the mitral valve complex. An experimental study. Eur J Cardiothorac Surg. 2007;32:96–101.
56. Komeda M, Glasson JR, Bolger AF, Daughters GT 2nd, Ingels NB Jr, Miller DC. Papillary muscle-left ventricular wall "complex". J Thorac Cardiovasc Surg. 1997;113:292–300; discussion 1.
57. Kono T, Sabbah HN, Rosman H, Alam M, Jafri S, Goldstein S. Left ventricular shape is the primary determinant of functional mitral regurgitation in heart failure. J Am Coll Cardiol. 1992;20:1594–8.
58. Messas E, Guerrero JL, Handschumacher MD, Chow CM, Sullivan S, Schwammenthal E, et al. Paradoxic decrease in ischemic mitral regurgitation with papillary muscle dysfunction: insights from three-dimensional and contrast echocardiography with strain rate measurement. Circulation. 2001;104:1952–7.
59. Lang RM, Mor-Avi V, Sugeng L, Nieman PS, Sahn DJ. Three-dimensional echocardiography: the benefits of the additional dimension. J Am Coll Cardiol. 2006;48:2053–69.
60. Delgado V, Tops LF, Schuijf JD, de Roos A, Brugada J, Schalij MJ, et al. Assessment of mitral valve anatomy and geometry with multislice computed tomography. JACC Cardiovasc Imaging. 2009;2:556–65.
61. Shanks M, Delgado V, Ng AC, van der Kley F, Schuijf JD, Boersma E, et al. Mitral valve morphology assessment: three-dimensional transesophageal echocardiography versus computed tomography. Ann Thorac Surg. 2010;90:1922–9.
62. Kaji S, Nasu M, Yamamuro A, Tanabe K, Nagai K, Tani T, et al. Annular geometry in patients with chronic ischemic mitral regurgitation: three-dimensional magnetic resonance imaging study. Circulation. 2005;112:I409–14.
63. Myerson SG. Heart valve disease: investigation by cardiovascular magnetic resonance. J Cardiovasc Magn Reson. 2012;14:7.
64. Enriquez-Sarano M, Miller FA Jr, Hayes SN, Bailey KR, Tajik AJ, Seward JB. Effective mitral regurgitant orifice area: clinical use and pitfalls of the proximal isovelocity surface area method. J Am Coll Cardiol. 1995;25:703–9.
65. Zoghbi WA, Enriquez-Sarano M, Foster E, Grayburn PA, Kraft CD, Levine RA, et al. Recommendations for evaluation of the severity of native valvular regurgitation with two-dimensional and Doppler echocardiography. J Am Soc Echocardiogr. 2003;16:777–802.

66. Adams DH, Rosenhek R, Falk V. Degenerative mitral valve regurgitation: best practice revolution. Eur Heart J. 2010;31:1958–66.
67. Garbi M, Monaghan MJ. Quantitative mitral valve anatomy and pathology. Echo Res Pract. 2015;2:R63–72.
68. Nishimura RA, Otto CM, Bonow RO, Carabello BA, Erwin JP 3rd, Guyton RA, et al. 2014 AHA/ACC guideline for the management of patients with valvular heart disease: executive summary: a report of the American College of Cardiology/American Heart Association Task Force on Practice Guidelines. J Am Coll Cardiol. 2014;63:2438–88.
69. Buck T, Plicht B, Kahlert P, Schenk IM, Hunold P, Erbel R. Effect of dynamic flow rate and orifice area on mitral regurgitant stroke volume quantification using the proximal isovelocity surface area method. J Am Coll Cardiol. 2008;52:767–78.
70. Adams DH, Anyanwu AC. The cardiologist's role in increasing the rate of mitral valve repair in degenerative disease. Curr Opin Cardiol. 2008;23:105–10.
71. Chikwe J, Adams DH, Su KN, Anyanwu AC, Lin HM, Goldstone AB, et al. Can three-dimensional echocardiography accurately predict complexity of mitral valve repair? Eur J Cardiothorac Surg. 2012;41:518–24.
72. Agricola E, Oppizzi M, Maisano F, De Bonis M, Schinkel AF, Torracca L, et al. Echocardiographic classification of chronic ischemic mitral regurgitation caused by restricted motion according to tethering pattern. Eur J Echocardiogr. 2004;5:326–34.
73. Calafiore AM, Di Mauro M, Gallina S, Di Giammarco G, Iaco AL, Teodori G, et al. Mitral valve surgery for chronic ischemic mitral regurgitation. Ann Thorac Surg. 2004;77:1989–97.
74. Silbiger JJ. Mechanistic insights into ischemic mitral regurgitation: echocardiographic and surgical implications. J Am Soc Echocardiogr. 2011;24:707–19.
75. Yiu SF, Enriquez-Sarano M, Tribouilloy C, Seward JB, Tajik AJ. Determinants of the degree of functional mitral regurgitation in patients with systolic left ventricular dysfunction: a quantitative clinical study. Circulation. 2000;102:1400–6.
76. Zoghbi WA, Adams D, Bonow RO, Enriquez-Sarano M, Foster E, Grayburn PA, et al. Recommendations for noninvasive evaluation of native valvular regurgitation: a report from the American Society of Echocardiography developed in collaboration with the Society for Cardiovascular Magnetic Resonance. J Am Soc Echocardiogr. 2017;30:303–71.
77. Hall SA, Brickner ME, Willett DL, Irani WN, Afridi I, Grayburn PA. Assessment of mitral regurgitation severity by Doppler color flow mapping of the vena contracta. Circulation. 1997;95:636–42.
78. Schwammenthal E, Chen C, Benning F, Block M, Breithardt G, Levine RA. Dynamics of mitral regurgitant flow and orifice area. Physiologic application of the proximal flow convergence method: clinical data and experimental testing. Circulation. 1994;90:307–22.
79. Biner S, Rafique A, Rafii F, Tolstrup K, Noorani O, Shiota T, et al. Reproducibility of proximal isovelocity surface area, vena contracta, and regurgitant jet area for assessment of mitral regurgitation severity. J Am Coll Cardiol Imaging. 2010;3:235–43.
80. Utsunomiya T, Ogawa T, Doshi R, Patel D, Quan M, Henry WL, et al. Doppler color flow "proximal isovelocity surface area" method for estimating volume flow rate: effects of orifice shape and machine factors. J Am Coll Cardiol. 1991;17:1103–11.
81. Zoghbi WA, Quinones MA. Determination of cardiac output by Doppler echocardiography: a critical appraisal. Herz. 1986;11:258–68.
82. Mascherbauer J, Rosenhek R, Bittner B, Binder J, Simon P, Maurer G, et al. Doppler echocardiographic assessment of valvular regurgitation severity by measurement of the vena contracta: an in vitro validation study. J Am Soc Echocardiogr. 2005;18:999–1006.
83. Khanna D, Vengala S, Miller AP, Nanda NC, Lloyd SG, Ahmed S, et al. Quantification of mitral regurgitation by live three-dimensional transthoracic echocardiographic measurements of vena contracta area. Echocardiography. 2004;21:737–43.
84. Kahlert P, Plicht B, Schenk IM, Janosi RA, Erbel R, Buck T. Direct assessment of size and shape of noncircular vena contracta area in functional versus organic mitral regurgitation using real-time three-dimensional echocardiography. J Am Soc Echocardiogr. 2008;21:912–21.
85. Otsuji Y, Handschumacher MD, Schwammenthal E, Jiang L, Song JK, Guerrero JL, et al. Insights from three-dimensional echocardiography into the mechanism of functional mitral regurgitation: direct in vivo demonstration of altered leaflet tethering geometry. Circulation. 1997;96:1999–2008.
86. Irvine T, Li XN, Rusk R, Lennon D, Sahn DJ, Kenny A. Three dimensional colour Doppler echocardiography for the characterisation and quantification of cardiac flow events. Heart. 2000;84(Suppl 2):II2–6.
87. Iwakura K, Ito H, Kawano S, Okamura A, Kurotobi T, Date M, et al. Comparison of orifice area by transthoracic three-dimensional Doppler echocardiography versus proximal isovelocity surface area (PISA) method for assessment of mitral regurgitation. Am J Cardiol. 2006;97:1630–7.
88. Song JM, Kim MJ, Kim YJ, Kang SH, Kim JJ, Kang DH, et al. Three-dimensional characteristics of functional mitral regurgitation in patients with severe left ventricular dysfunction: a real-time three-dimensional colour Doppler echocardiography study. Heart. 2008;94:590–6.
89. Picano E, Pibarot P, Lancellotti P, Monin JL, Bonow RO. The emerging role of exercise testing and stress echocardiography in valvular heart disease. J Am Coll Cardiol. 2009;54:2251–60.
90. Lancellotti P, Gerard PL, Pierard LA. Long-term outcome of patients with heart failure and dynamic functional mitral regurgitation. Eur Heart J. 2005;26:1528–32.
91. Ray S. The echocardiographic assessment of functional mitral regurgitation. Eur J Echocardiogr. 2010;11:i11–7.